

A functional genomics screen identifies PCAF and ADA3 as regulators of human granzyme B-mediated apoptosis and Bid cleavage

D Brasacchio^{1,2}, T Noori^{1,2}, C House^{1,2}, AJ Brennan^{1,2}, KJ Simpson^{1,3}, O Susanto^{1,2,4}, PI Bird⁵, RW Johnstone^{*,1,6,7} and JA Trapani^{*,1,2,7}

The human lymphocyte toxins granzyme B (hGrzB) and perforin cooperatively induce apoptosis of virus-infected or transformed cells: perforin pores enable entry of the serine protease hGrzB into the cytosol, where it processes Bid to selectively activate the intrinsic apoptosis pathway. Truncated Bid (tBid) induces Bax/Bak-dependent mitochondrial outer membrane permeability and the release of cytochrome c and Smac/Diablo. To identify cellular proteins that regulate perforin/hGrzB-mediated Bid cleavage and subsequent apoptosis, we performed a gene-knockdown (KD) screen using a lentiviral pool of short hairpin RNAs embedded within a miR30 backbone (shRNAmiR). We transduced HeLa cells with a lentiviral pool expressing shRNAmiRs that target 1213 genes known to be involved in cell death signaling and selected cells with acquired resistance to perforin/hGrzB-mediated apoptosis. Twenty-two shRNAmiRs were identified in the positive-selection screen including two, PCAF and ADA3, whose gene products are known to reside in the same epigenetic regulatory complexes. Small interfering (si)RNA-mediated gene-KD of PCAF or ADA3 also conferred resistance to perforin/hGrzB-mediated apoptosis providing independent validation of the screen results. Mechanistically, PCAF and ADA3 exerted their pro-apoptotic effect upstream of mitochondrial membrane permeabilization, as indicated by reduced cytochrome c release in PCAF-KD cells exposed to perforin/hGrzB. While overall levels of Bid were unaltered, perforin/hGrzB-mediated cleavage of Bid was reduced in PCAF-KD or ADA3-KD cells. We discovered that PCAF-KD or ADA3-KD resulted in reduced expression of PACS2, a protein implicated in Bid trafficking to mitochondria and importantly, targeted PACS2-KD phenocopied the effect of PCAF-KD or ADA3-KD. We conclude that PCAF and ADA3 regulate Bid processing via PACS2, to modulate the mitochondrial cell death pathway in response to hGrzB.

Cell Death and Differentiation (2014) 21, 748–760; doi:10.1038/cdd.2013.203; published online 24 January 2014

Human GrzB (hGrzB) is a pro-apoptotic protease that induces target cell death by activating the mitochondrial (intrinsic) cell death pathway in a perforin-dependent manner.^{1–5} Like caspases, hGrzB processes substrate proteins after key aspartate residues ('asp-ase activity'), but with substantially different fine substrate specificity. After entry into the target cell cytoplasm, a key early step is cleavage of the BH3 domain-only protein Bid at a dedicated hGrzB site (Asp-75), distinct from the caspase site (Asp60).^{6,7} Translocation of truncated Bid (tBid) to mitochondria results in destabilization and permeabilization of mitochondrial outer membrane (MOMP) and release of cytochrome c and Smac/Diablo from the intermembrane space. Caspase activation through the mitochondrial pathway is a hallmark of hGrzB: although the granzyme can directly initiate the processing of pro-caspase-3

(and several other effector caspases), minimal caspase activity results as further auto-processing of pro-caspase-3 occurs only when Smac/Diablo displaces inhibitor of apoptosis proteins (IAP's) from the partly processed pro-caspases. Smac/Diablo release also induces apoptosome formation that activates caspase-9. Overexpression of Bcl-2 (Bcl-2-overexpression) or its viral orthologue BHRF1 in human cells very effectively blocks hGrzB, as they inhibit MOMP, resulting in cytochrome c and Smac/Diablo retention within mitochondria.^{8,9} By contrast, subtle species differences in proteolytic specificity dictate that mouse GrzB preferentially activate pro-caspases directly, rather than cleaving Bid.^{1,10} Mouse GrzB is therefore less prone to inhibition by Bcl-2 and like inhibitors.¹

The fact that Bcl-2-overexpression confers both short-term resistance to perforin/hGrzB and enables long term

¹Sir Peter MacCallum Department of Oncology, The University of Melbourne, Parkville, VIC, Australia; ²Cancer Immunology Program, Peter MacCallum Cancer Centre, East Melbourne, VIC, Australia; ³Victorian Centre for Functional Genomics, Peter MacCallum Cancer Centre, East Melbourne, VIC, Australia; ⁴The Beatson Institute for Cancer Research, Glasgow, UK; ⁵Department of Biochemistry and Molecular Biology, School of Biomedical Sciences, Monash University, Clayton, VIC, Australia and ⁶Cancer Therapeutics Program, Peter MacCallum Cancer Centre, East Melbourne, VIC, Australia

*Corresponding author: RW Johnstone, Peter MacCallum Cancer, St Andrew's Place, East Melbourne 3002, Australia. Tel: +613 9656 3727; Fax: +613 9656 1411; E-mail: ricky.johnstone@petermac.org

or JA Trapani, Peter MacCallum Cancer Centre, St Andrew's Place, East Melbourne 3002, Australia. Tel: +613 9656 1516; Fax: +613 9656 1414; E-mail: joe.trapani@petermac.org

⁷These authors contributed equally to this work.

Keywords: granzyme B; perforin; cell death; PCAF; ADA3; Bid

Abbreviations: hGrzB, human granzyme B; tBid, truncated Bid; KD, knockdown; MOMP, mitochondrial outer membrane permeabilization; IAP, inhibitor of apoptosis protein; CTLs, cytotoxic lymphocytes; NK, natural killer cell; PCAF, p300/CBP associated protein; ADA3, transcriptional adaptor 3; PACS2, phosphofurin acidic-cluster sorting-protein 2; NS, non-silencing; AB, Alamar blue; NT, non-targeting; UV, ultraviolet radiation; CSP3, caspase-3; IP, immunoprecipitation

Received 17.9.13; revised 15.12.13; accepted 16.12.13; Edited by H-U Simon; published online 24.1.14

clonogenic survival indicates that Bid-mediated MOMP is the dominant cell death signaling pathway activated by hGrzB. This is also borne out kinetically: Bid cleavage occurs within 60 s of hGrzB accessing the cytosol and MOMP follows in as little as 3–5 min.¹¹ Nonetheless, a variety of studies have shown that hGrzB can also cleave other intracellular proteins with variable efficiency, and it is likely that some (or perhaps many) may have physiological relevance, including filamin, gelsolin and ROCKII.^{12–14} Many viruses express Bcl-2-like proteins, and we have shown that the EBV orthologue BHRF1 is a potent blocker of hGrzB-mediated cell death. Despite this, intact cytotoxic lymphocytes (CTLs) (as distinct from purified recombinant reagents) are able to circumvent a Bcl-2-like block,⁸ indicating that alternative pathways to cell death must exist.

Given the dominant role of hGrzB in human CTLs or natural killer (NK) cell-mediated cell death and the plethora of putative substrates, further understanding the mechanisms involved in hGrzB-induced death is of great importance. We chose to investigate this by performing a gain-of-representation gene-knockdown screen that examined the impact of knockdown of ~1213 genes reported to have a role in programmed cell death. Amongst 22 genes reproducibly identified in the screen, we identified epigenetic regulators p300/CBP associated protein (PCAF) and transcriptional adaptor 3 (ADA3), known to interact within the same macromolecular complex, as regulators of perforin/hGrzB-mediated Bid cleavage and intrinsic apoptosis. Further mechanistic insight was provided by our discovery that knockdown of a potential downstream target gene of PCAF and ADA3, phosphofurin acidic-cluster sorting-protein 2 (PACS2), also resulted in reduced Bid cleavage and apoptosis following treatment with perforin/hGrzB. Our studies therefore identified a novel integrated molecular pathway that regulates a cell's susceptibility to perforin/hGrzB.

Results

A functional genomics screen identifies genes that regulate perforin/hGrzB-mediated apoptosis. A library of ~4000 shRNAmiRs directed against 1213 genes (Supplementary Table 1) previously involved in cell death were pooled, packaged into lentivirus and used to transduce HeLa cervical cancer cells (HeLa) (Supplementary Figure 1). Given significant species differences in substrate specificity, all of our experiments (both in the initial screen and all subsequent studies) utilized only human target cells and hGrzB. Stably transduced HeLa were selected by growth in medium containing puromycin. A low multiplicity of viral infection that favored single lentivirus integration per cell was used, resulting in ~20% of the starting population acquiring puromycin resistance and expressing the GFP reporter protein (data not shown). After recovering for 48 h and resuming proliferation in selective medium, cells were exposed to a normally lethal concentration of recombinant hGrzB (60 nM), combined with a sublytic quantity of recombinant perforin (1 nM). This concentration of hGrzB was chosen as it is sufficient to induce >80% specific ⁵¹Cr release from non-silencing (NS)-shRNAmir transduced control cells in a standard 4-hour assay, or render >80% of cells permeable

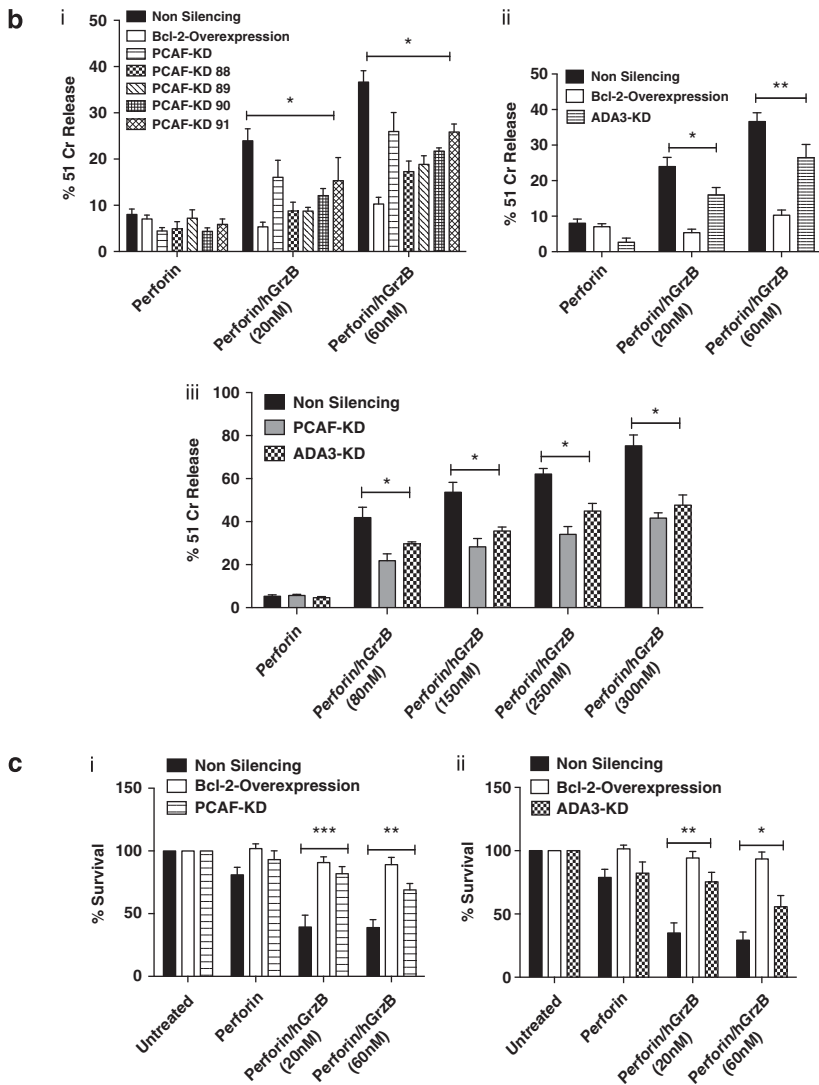
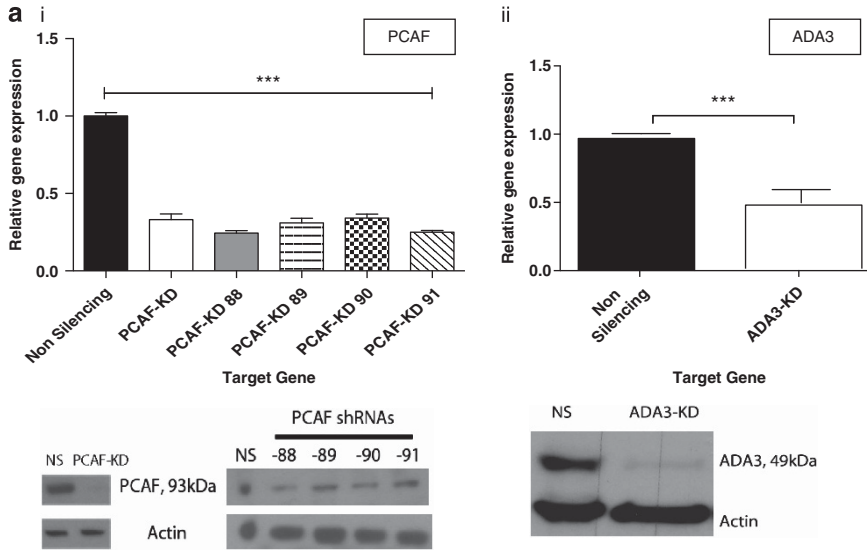
to the vital dye Alamar blue (AB) 24 h after treatment (data not shown). By contrast, the same concentration of perforin applied alone produced <10% specific ⁵¹Cr release and had no significant effect on long-term viability (data not shown). To select for cells that had acquired resistance to perforin/hGrzB, pools of transduced HeLa were expanded and exposed to three further rounds of selection (Supplementary Figure 1), to produce cell populations significantly resistant to hGrzB-induced apoptosis (Hit 4), compared with NS controls ($P < 0.05$, Supplementary Figure 2a).

To identify specific shRNAmiRs that conferred resistance to perforin/hGrzB, the pool of resistant cells was cloned and DNA was extracted for sequencing. We identified 25 shRNAmiRs targeting 22 candidate genes. Two different shRNAmiRs targeting GTF2H3, MAPK8 and TGFBR1 were identified in the original screen (Supplementary Figure 2b). To validate the candidate genes, HeLa expressing the same individual shRNAmiRs as identified in the screen, were exposed to perforin/hGrzB (60 nM) (Supplementary Figure 2c). As Bcl-2-overexpression powerfully suppresses hGrzB-mediated death,⁸ Bcl-2-overexpressing HeLa were used as controls (Supplementary Figure 2c). When knocked down, five gene candidates displayed consistent resistance to perforin/hGrzB (PCAF, ADA3, YWHAQ, PKR and WDR33). A further validation step was performed using shRNAmiRs directed to different regions of the gene sequences (Supplementary Figure 2di). The results consistently showed that KD of PCAF, ADA3, YWHAQ, PKR and WDR33 provided significant resistance to perforin/hGrzB-mediated apoptosis ($P < 0.001$, Supplementary Figure 2di). Furthermore, protection conferred by the depletion of these five candidates was comparable with Bcl-2 overexpression, (Supplementary Figure 2di). To confirm our findings, an independent technology, siRNA-mediated gene KD was used. Once again, depletion of PCAF, ADA3, YWHAQ, PKR and WDR33 provided reproducible and statistically significant suppression of apoptosis when compared with siRNA for a non-targeting (NT) region or GAPDH-KD ($P < 0.001$, Supplementary Figure 2dii).

Reduced expression of PCAF or ADA3 confers resistance to perforin/hGrzB.

To further test the robustness of our findings, four additional shRNAs targeting different regions of the PCAF mRNA and the ADA3 shRNA, were examined. PCAF shRNAs PCAF, -88, -89, -90 and -91 reduced steady-state PCAF protein, albeit at varying levels depending on the shRNA, and all significantly reduced mRNA levels by ~75% compared with NS ($P < 0.001$, Figure 1ai). ADA3 mRNA and protein were also significantly reduced by the ADA3 shRNA ($P < 0.001$, Figure 1aii). All five PCAF shRNAs and the ADA3 shRNA, protected HeLa from perforin/hGrzB in 4 h ⁵¹Cr release assays (Figures 1bi–iii), while long-term cell viability (AB exclusion at 24 h, and continued proliferation) was also observed to a similar level as Bcl-2 overexpression (Figures 1ci and ii). Similar results were also achieved with individual siRNAs targeting PCAF or ADA3 (Supplementary Figure 3b and c).

PCAF is a transcriptional co-factor that acetylates histone and non-histone proteins,^{15,16} while ADA3 is an important transcriptional adaptor protein that binds to PCAF in both the hSAGA and ATAC complexes.¹⁷ The fact that PCAF and



ADA3 had been independently identified in our screen strongly suggested a novel epigenetic/transcriptional mechanism was responsible for regulating sensitivity to perforin/hGrzB. If PCAF and ADA3 operate in the same signaling pathways,¹⁷ we predicted that reducing the levels of both would have no greater effect than suppressing either alone. We found it difficult to maintain cell viability when both genes were suppressed at similar levels as achieved individually (data not shown). Ultimately, we produced cells in which PCAF expression was reduced by ~50% and ADA3 by ~25% (Figure 2ai-ii), but protection against perforin/hGrzB was not further enhanced (Figure 2b).

How does suppressing PCAF levels endow protection against hGrzB? We sought to determine whether PCAF was exerting its effect on perforin/hGrzB-mediated death upstream or downstream of MOMP.^{3,6,18,19} The release of cytochrome c was markedly reduced in cells with down-regulated PCAF, whereas the broad-spectrum caspase inhibitor Q-VD-OPh (QVD), which exerts its effect downstream of MOMP, did not enhance protection (Figure 3). This indicated that protection was occurring at or proximal to the mitochondria. We examined steady-state mRNA and protein levels for Bid and mRNA levels for Bcl-2, but neither was significantly changed (Supplementary Figures 4a and bi), nor were mRNA levels of other Bcl-2 family members (Mcl-1, Bcl-xl) (Supplementary Figures 4bii-iv). A significant increase in Bcl-w expression was also observed but was insufficient to impart protection. In other studies, the pro-survival effect of Bcl-w has been shown to be restricted to sperm and epithelial cells derived from the gut.^{20,21} Extending this 'candidate' approach, we also found normal levels of mRNA and protein for Smac/Diablo, Bax and cytochrome c (data not shown). We next examined whether PCAF- or ADA3-KD conferred protection against other death stimuli that operate through the mitochondrial pathway. Ligation of the death receptor TRAIL initiates apoptosis through the apical procaspase-8 (or occasionally, -10) and is negatively regulated by Bcl-2 in a cell line-specific manner.^{22,23} HeLa with downregulated PCAF or ADA3 were not protected against TRAIL and continued to process pro-caspases-8 and -3 normally, whereas Bcl-2 overexpression strongly suppressed cell death (Figures 4ai and ii and bi and ii and Supplementary Figure 5d). Results were similar when we exposed the same cells to ultraviolet radiation (UV), which also activates the mitochondrial cell death pathway²⁴ (Figure 4ci-ii and Supplementary Figure 5e).

Reduced Bid processing in HeLa cells depleted of PCAF or ADA3. Due to the significant reduction in cytochrome c release in PCAF-depleted HeLa (Figure 3), we investigated the potential involvement of Bid in its direct processing as hGrzB is a pivotal initiating step leading to MOMP^{1,4,6} and the removal of Bid has been shown to mediate resistance to perforin/hGrzB.^{6,25} We generated Bid-depleted HeLa (Bid-KD) (Supplementary Figure 5a) and found they displayed similar levels of resistance to perforin/hGrzB-mediated cell death as PCAF-KD or ADA3-KD cells, compared with NS controls (Supplementary Figure 5c, $P < 0.001$). Bid-KD also showed incomplete caspase-3 (CSP3) processing from p20 to p17 following exposure to perforin/hGrzB and, similar to PCAF-KD cells, decreased cytochrome c release compared with NS (Supplementary Figures 5a and b). These similarities between Bid-KD and PCAF- or ADA3-KD cells upon perforin/hGrzB treatment suggested that Bid processing may be affected in PCAF- or ADA3-KD cells. Although we have shown Bid mRNA and protein levels were not reduced as a result of PCAF or ADA3 depletion (Supplementary Figure 4a), we assessed Bid processing in these cells. We found a significant reduction of Bid processing when either PCAF or ADA3 was depleted (Figures 5a-c), even when high concentrations of hGrzB (100 nM) were used (Figure 5c). This was also seen in HCT116 colon cancer cells when depleted of PCAF or ADA3, particularly in PCAF-KD cells (Supplementary Figure 7b). The slightly slower-migrating caspase-cleaved tBid was also observed, and was lost with the addition of QVD, with minimal effect on the hGrzB-cleaved form (Figures 5a and b). Reduced Bid cleavage was also evident in cells depleted of both PCAF and ADA3 (Figure 5d).

It was possible that ADA3 and/or PCAF might transcriptionally regulate Bid processing by affecting expression of the cognate hGrzB inhibitor SERPIN-B9 (formerly known as PI9).²⁶ However, SERPIN-B9 mRNA and protein levels were not altered in PCAF- or ADA3-depleted cells (Supplementary Figure 6a). To test for an alternate direct hGrzB inhibitor (although none has ever been described), purified recombinant hGrzB was incubated with graded amounts of lysate from NS, PCAF- or ADA3-depleted HeLa. The inhibitory effect of PCAF- or ADA3-depleted HeLa cell lysate on hGrzB's proteolytic activity was similar to control (Supplementary Figures 6bi and ii and data not shown). In addition, we found no variation in perforin-dependent hGrzB internalization in NS, PCAF or ADA3-depleted cells (Supplementary Figure 6c).

Figure 1 Reduction in PCAF or ADA3 expression by shRNA leads to resistance to perforin/hGrzB-mediated cell death. (a) HeLa were transfected with shRNA targeting non-silencing (NS), PCAF or ADA3. Five PCAF shRNA (PCAF, PCAF-88, PCAF-89, PCAF-90, PCAF-91) were used which target different areas of the PCAF gene where PCAF refers to the shRNA identified from the original screen (Supplementary Figure 2). Determination of gene and protein knockdown of i. PCAF and ii. ADA3 in HeLa. For gene detection, RNA was extracted and relative mRNA expression of PCAF or ADA3 in HeLa was measured by qRT-PCR. Protein detection was observed by subjecting whole-cell lysates to immunoblot for PCAF or ADA3 with Actin serving as a protein loading control. (b) HeLa with shRNA-mediated depletion of PCAF or ADA3 were suppressed from perforin/hGrzB-mediated death after 4 h. HeLa with KD of PCAF, ADA3 or non-silencing compared with stable Bcl-2-overexpressing cells, were treated with sublytic perforin in the absence or presence of hGrzB at 20 nM or 60 nM and a 4 h ⁵¹Cr release assay performed. ⁵¹Cr release for i. PCAF-KD or ii. ADA3-KD cells compared with non-silencing or Bcl-2-overexpression HeLa and iii. Perforin/hGrzB titration of PCAF-KD or ADA3-KD cells compared with non-silencing HeLa. (c) HeLa with shRNA-mediated depletion of PCAF or ADA3 were suppressed from perforin/hGrzB-mediated death after 24 h. HeLa with KD of PCAF, ADA3 or non-silencing compared with stable Bcl-2-overexpressing cells, were treated with sublytic perforin in the absence or presence of hGrzB at 20 nM and 60 nM and an AB viability assay performed at 24 h. AB exclusion for i. PCAF-KD or ii. ADA3-KD cells compared with the non-silencing or Bcl-2-overexpression HeLa. Error bars represent S.E.M., $n = 3$. Statistical analysis performed: one-way ANOVA versus non-silencing and a Bonferroni test, * $P < 0.05$, ** $P < 0.01$ and *** $P < 0.001$. Immunoblots are a representative of three independent experiments

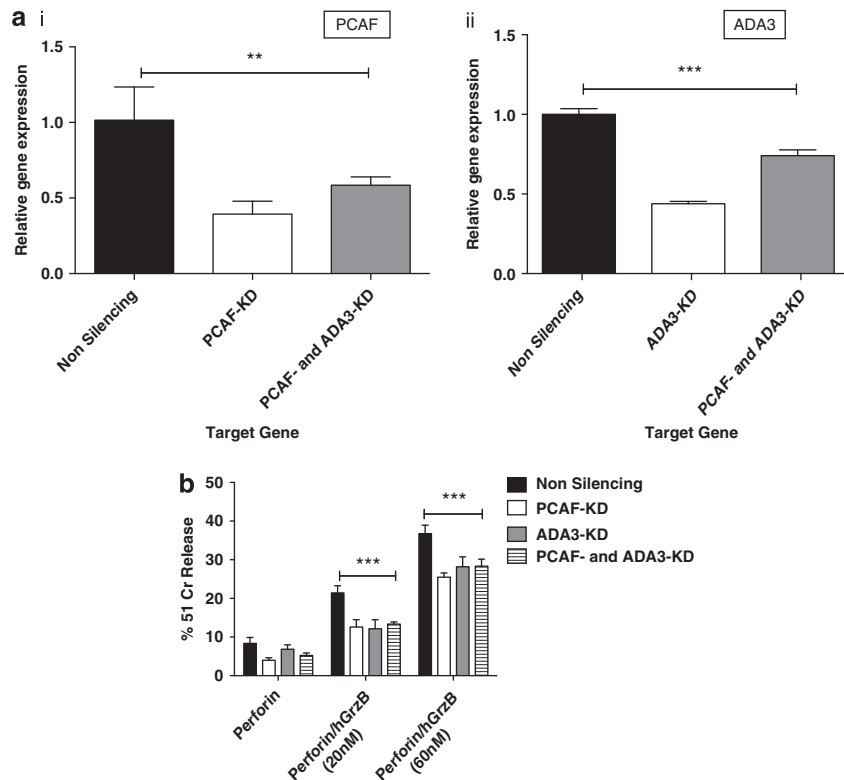


Figure 2 Combined PCAF and ADA3 knockdown maintains resistance to perforin/hGrzB-mediated cell death. (a) HeLa transduced with both PCAF and ADA3 shRNA (PCAF- and ADA3-KD) had reduced expression of both PCAF and ADA3. RNA was extracted from non-silencing, PCAF-KD, ADA3-KD and PCAF- and ADA3-KD HeLa and relative mRNA expression was detected by qRT-PCR. i. PCAF gene expression for non-silencing, PCAF-KD, PCAF- and ADA3-KD. ii. ADA3 gene expression for non-silencing, ADA3-KD, PCAF- and ADA3-KD. (b) HeLa with PCAF- and ADA3-KD was suppressed from perforin/hGrzB-mediated cell death similar to PCAF-KD or ADA3-KD cells. HeLa non-silencing, PCAF-KD, ADA3-KD or PCAF- and ADA3-KD were treated with sublytic perforin in the absence or presence of hGrzB at 20 nM or 60 nM and a 4 h ^{51}Cr release assay completed. Error bars represent S.E.M., $n = 3$. Statistical analysis performed: one way ANOVA versus non-silencing and a Bonferroni test, $**P < 0.01$ and $***P < 0.001$

Another possibility was PCAF or ADA3 directly catalyzed hGrzB's cleavage of Bid, by directly associating with Bid. We considered this unlikely, as Bid is localized in the cytosol, whereas PCAF and ADA3 are typically nuclear proteins. Nonetheless, PCAF may shuttle between the nucleus and cytosol under certain circumstances.²⁷ We formally excluded this possibility in two ways: first, we used co-immunoprecipitation (IP) to show that, as expected, ADA3 and PCAF form a complex (Figure 6a and data not shown) with one another, but this did not include Bid (Figures 6bi and ii). Reciprocal immunoprecipitations using antibodies specific for Bid showed Bid did not co-precipitate PCAF (Figure 6biii) or ADA3 (data not shown). Second, we examined the subcellular localization of ADA3 and PCAF, both constitutively and following exposure to lethal concentrations of perforin/hGrzB. Immunoblot analysis demonstrated that PCAF and ADA3 were located in the nuclear fraction of lysed HeLa while Bid remained in the cytosol (Figures 6ci and ii). PCAF remained nuclear, both constitutively and when the cells were incubated with perforin/hGrzB (Figure 6ciii). These findings were also confirmed for PCAF by immunofluorescence staining (Figures 6di and ii).

Is Bid post-translationally modified in the presence or absence of PCAF or ADA3? We considered whether gene

regulatory activities of PCAF or ADA3 might affect Bid processing by influencing post-translational modifications of full-length Bid, or through modified clearance of its pro-apoptotic cleavage products. For example, phosphorylation of mouse Bid on Ser61, Ser64 or Thr59 flanking the caspase cleavage site (Asp60) can inhibit Bid processing by caspase-8 or -3.^{7,28} Furthermore, Ser-78 adjacent to the dedicated hGrzB cleavage site can be transiently phosphorylated in response to DNA double-strand breaks.²⁹ However, we detected no change in Ser78 phosphorylation in PCAF-depleted cells in either the absence or presence of perforin/hGrzB (Figure 7a, upper 2 panels); by contrast, Etoposide-treated HeLa displayed pronounced Ser78 phosphorylation. Phosphorylation of Ser65 also did not change with perforin/hGrzB exposure (Figure 7a, middle panel) and cleavage of Bid persisted (Figure 7a, lower panels). Furthermore, inhibiting proteasomal degradation of tBid with Bortezomib did not affect reduced tBid levels in PCAF-depleted cells (Figure 7b), ruling out accelerated tBid degradation as the mechanism of enhanced protection.

PCAF or ADA3 depletion results in reduced PACS2 expression and PACS2 depletion phenocopies reduced Bid processing. Transport of Bid to the mitochondria is an important step leading to oligomerization of Bax/Bak to

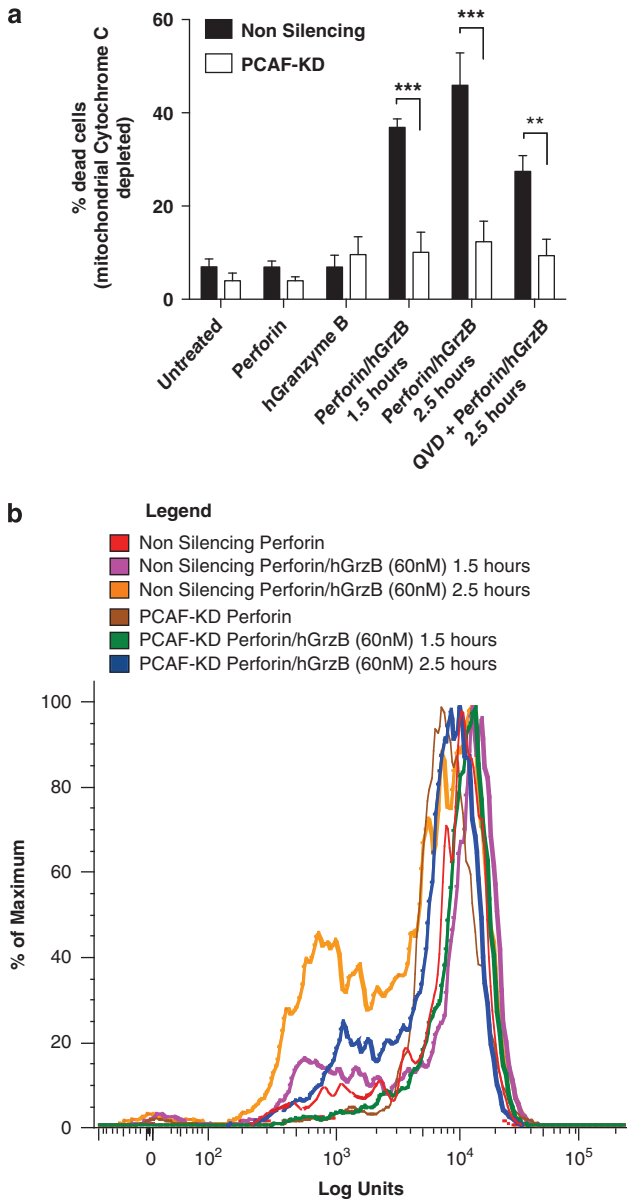


Figure 3 PCAF depletion leads to suppression of perforin/hGrzB-mediated mitochondrial cytochrome c release. Cytochrome c release of HeLa PCAF-KD cells is reduced. HeLa non-silencing or PCAF-KD cells were treated with perforin in the absence or presence of hGrzB (60 nM) or QVD (10 μ M) for the indicated times then analyzed for cytochrome c staining by FACS. **(a)** Bar chart representing cytochrome c stained cells for HeLa PCAF-KD compared with non-silencing. **(b)** The panels show FACS overlays of non silencing or PCAF-KD cells. The X axis depicts log units and represents the level of cytochrome c-stained cells. A reduction in units indicates a loss of cytochrome c from the mitochondria. Error bars represent S.E.M., $n = 3$. Statistical analysis performed: one way ANOVA versus non silencing and a Bonferroni test, ** $P < 0.01$ and *** $P < 0.001$

initiate MOMP,^{3,30} and this in turn requires PACS2, which binds unprocessed Bid.³¹ PACS2-Bid binding is enhanced following Fas ligation, and conversely, depletion of PACS2 leads to decreased Bid processing.³¹ Given that PCAF and ADA3 are transcriptional co-activators,^{15–17} we determined whether depletion of PCAF or ADA3 affected PACS2 expression. We found a significant reduction ($P < 0.01$) in PACS2 expression in PCAF- and ADA3-depleted HeLa and

HCT116 cells (Figure 8a and Supplementary Figure 7c). Next we used an shRNA directed against PACS2 to determine whether a reduction in PACS2 expression (Figure 8b) was sufficient to induce resistance to perforin/hGrzB-mediated cell death. PACS2 depletion led to significant protection against perforin/hGrzB ($P < 0.01$), as demonstrated by reduced ⁵¹Cr release (Figure 8ci). Furthermore, PACS2-KD also reduced Bid processing following perforin/hGrzB exposure (Figure 8cii).

Discussion

Immune-mediated death of infected or transformed human cells follows exocytic release of the serine protease GrzB that rapidly accesses the target cell cytosol via perforin pores.¹¹ The proteolytic processing of Bid to active tBid is a pivotal step initiating intrinsic apoptotic pathway, triggering MOMP and subsequent release of cytochrome c and Smac/Diablo.^{3–6,18} Further elucidating perforin/hGrzB-mediated cell death was warranted to aid our understanding of how diseased cells evade death. We performed a knockdown screen targeting 1213 genes associated with cell death signaling and selected candidates whose loss suppressed perforin/hGrzB-mediated apoptosis. Among 22 genes identified from the screen, we found that loss of either PCAF or ADA3, two proteins that associate within the same epigenetic regulating complexes,¹⁷ resulted in cell survival. The sustained resistance to cell death resulting from PCAF or ADA3 deficiency mapped upstream of mitochondria, as indicated by reduced cytochrome c release in response to perforin/hGrzB; in turn, this was associated with reduced cleavage/processing of Bid by hGrzB.

PCAF and ADA3 associate in the same signaling complexes to epigenetically regulate gene transcription.¹⁷ We systematically ruled out several resistance mechanisms that might have been recruited following PCAF- or ADA3-depletion: we found no evidence that a hGrzB inhibitor was induced, and specifically ruled out the irreversible, cognate serpin inhibitor SERPIN-B9. The expression levels of anti-apoptotic Bcl-2 family proteins was unaltered, and there was no evidence that either PCAF or ADA3, reported to shuttle to the cytoplasm under certain circumstances, interact directly with Bid to facilitate its cleavage; rather, as reported previously PCAF and ADA3 co-precipitated with each other (but not with Bid) and remained localized in nuclei of both healthy and dying cells. Suppression of cell death was observed to be hGrzB specific, as apoptosis mediated by TRAIL or UV, which rely on caspase processing^{23,24} was not affected. HeLa are 'Type II' cells that use the intrinsic pathway for TRAIL-mediated death, as shown by the fact that Bcl-2 overexpression results in protection.^{32,33} It is not clear why PCAF/ADA3 depletion failed to protect against TRAIL (even at low concentrations); however, it appears activated caspase-8 remains capable of directly activating caspase-3 when Bid processing is reduced. We sought to understand the mechanism(s) of reduced Bid processing in PCAF- or ADA3-depleted cells, but identified no change in its phosphorylation status, reported to influence its processing by caspases.^{28,29} Of particular importance, we confirmed that Ser-78, located close to the hGrzB Bid-cleavage site (Asp-75), was phosphorylated in response to the DNA-damaging agent etoposide²⁹ but not after

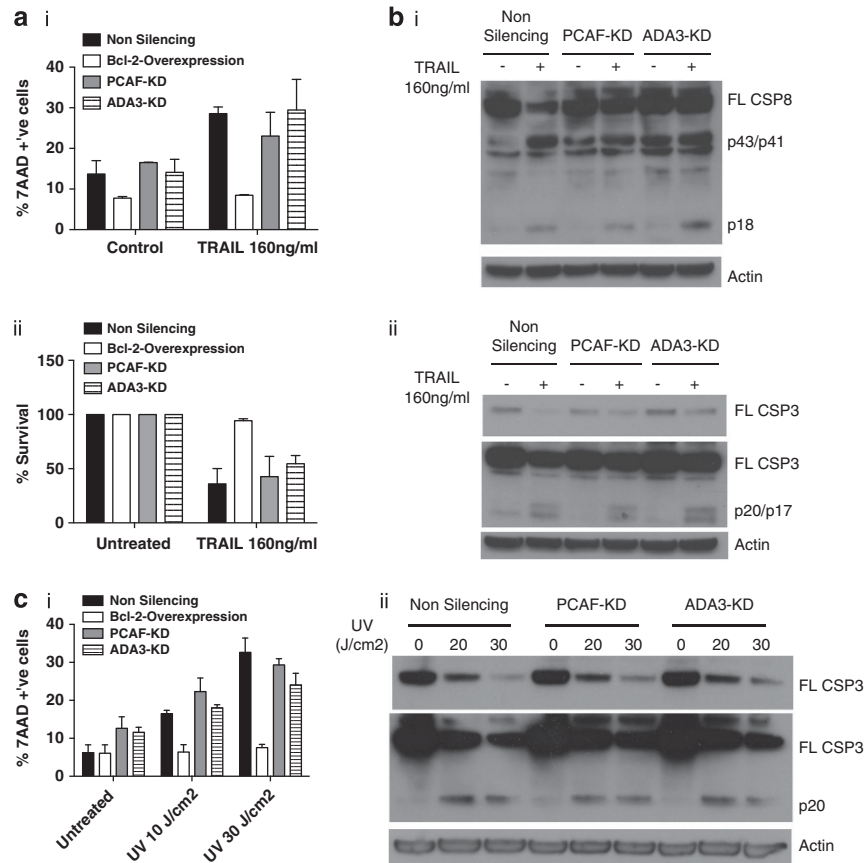


Figure 4 PCAF-KD or ADA3-KD HeLa are sensitive to TRAIL and UV light treatment. (a) PCAF-KD or ADA3-KD HeLa are sensitive to TRAIL treatment similar to non-silencing cells while Bcl-2-overexpression cells remain resistant. Non-silencing, PCAF-KD, ADA3-KD or Bcl-2-overexpression cells were treated with TRAIL (160 ng/ml), and cultured for 16 h and assessed for cell viability by i. 7-AAD staining and FACS, a bar chart shows the % 7-AAD positive cells or ii. AB exclusion assay. (b) PCAF-KD or ADA3-KD HeLa have caspase processing following TRAIL treatment similar to non-silencing cells. Non-silencing, PCAF-KD, ADA3-KD or Bcl-2-overexpression cells were treated with TRAIL (160 ng/ml), cultured for 16 h and assessed for caspase processing. Whole-cell lysates were subjected to immunoblot and probed for i. caspase-8 (CSP8); full length (FL); activated (p43/p41); or cleaved (p18) and ii. Caspase-3 (CSP3); full length (FL), processed (p20) or cleaved (p17). A lighter FL CSP3 (upper panel) is also presented. Total protein was evaluated by probing for Actin. (c) PCAF-KD or ADA3-KD HeLa are sensitive to UV light similar to non-silencing cells while Bcl-2-overexpression cells remain resistant. Non-silencing, PCAF-KD, ADA3-KD or Bcl-2-overexpressing cells were subjected to UV light treatment for 10, 20 or 30 joules/cm² (J/cm²) cultured for 16 h and assessed for cell viability and caspase processing. i. 7-AAD staining and FACS, a bar chart shows the % 7-AAD positive cells. ii. Caspase-3 processing assessment by subjecting whole-cell lysates to immunoblot for caspase-3 (CSP3) full length (FL) and processed (p20). The upper panel shows a lightly exposed FL CSP3 blot. Total protein was evaluated by probing for Actin. Error bars represent S.E.M., *n* = 3. Immunoblots are a representative of 3 independent experiments

perforin/hGrzB exposure. PCAF has been shown to have ubiquitinase activity,³⁴ but blocking the proteasome with Bortezomib did not affect tBid degradation.

Trafficking of dephosphorylated Bid to mitochondria is enhanced following extrinsic cell death activation with anti-Fas antibody³¹ and is regulated by the transporter PACS2. Indeed, PACS2-KD reduced Bid processing following Fas receptor cross-linking.³¹ We showed for the first time that PACS2 expression was reduced in PCAF- or ADA3-depleted cells, suggesting that PACS2 is a downstream target of PCAF and/or ADA3.¹⁷ Furthermore, independent knockdown of PACS2, conferred resistance to perforin/hGrzB and phenocopied reduced processing of Bid observed in PCAF- or ADA3-depleted cells. Our studies therefore identified a novel integrated molecular pathway regulating the target cell's response to perforin/hGrzB (Figure 8d).

Our findings provide important new information on cellular processes that regulate responses to primary apoptotic effector proteins of cytotoxic lymphocytes. Reinforcing the

dominance of the hGrzB signaling pathway, we recently showed pro-apoptotic granzymes act in a hierarchical fashion, recruiting diverse cell death pathways that all rely on access to the cell cytosol via perforin pores. Thus, in the absence of GrzB, cell death phenotype reverts to a slower, non-apoptotic cell death pathway ('athetosis'), in which GrzA targets the actin cytoskeleton.³⁵ This diversity and lack of reliance on a single death pathway are important for understanding how mammalian immune systems have stayed ahead in the evolutionary 'arms race' against intracellular pathogens. The literature records several ways in which hGrzB pathway may be blocked by viruses, including direct inhibition *in vitro* of GrzB by overexpressed viral serpins,³⁶ or by the capsid proteins of human adenovirus V,³⁷ or by elaboration of Bcl-2-like inhibitors such as Epstein-Barr virus BHRF1 to block signaling at the mitochondrion.⁹ In human cancer, the cognate hGrzB inhibitor SERPIN-B9 may be ectopically expressed to blunt CTL-mediated tumor cell attack.³⁸ Our identification of an epigenetic mechanism through which sensitivity to hGrzB

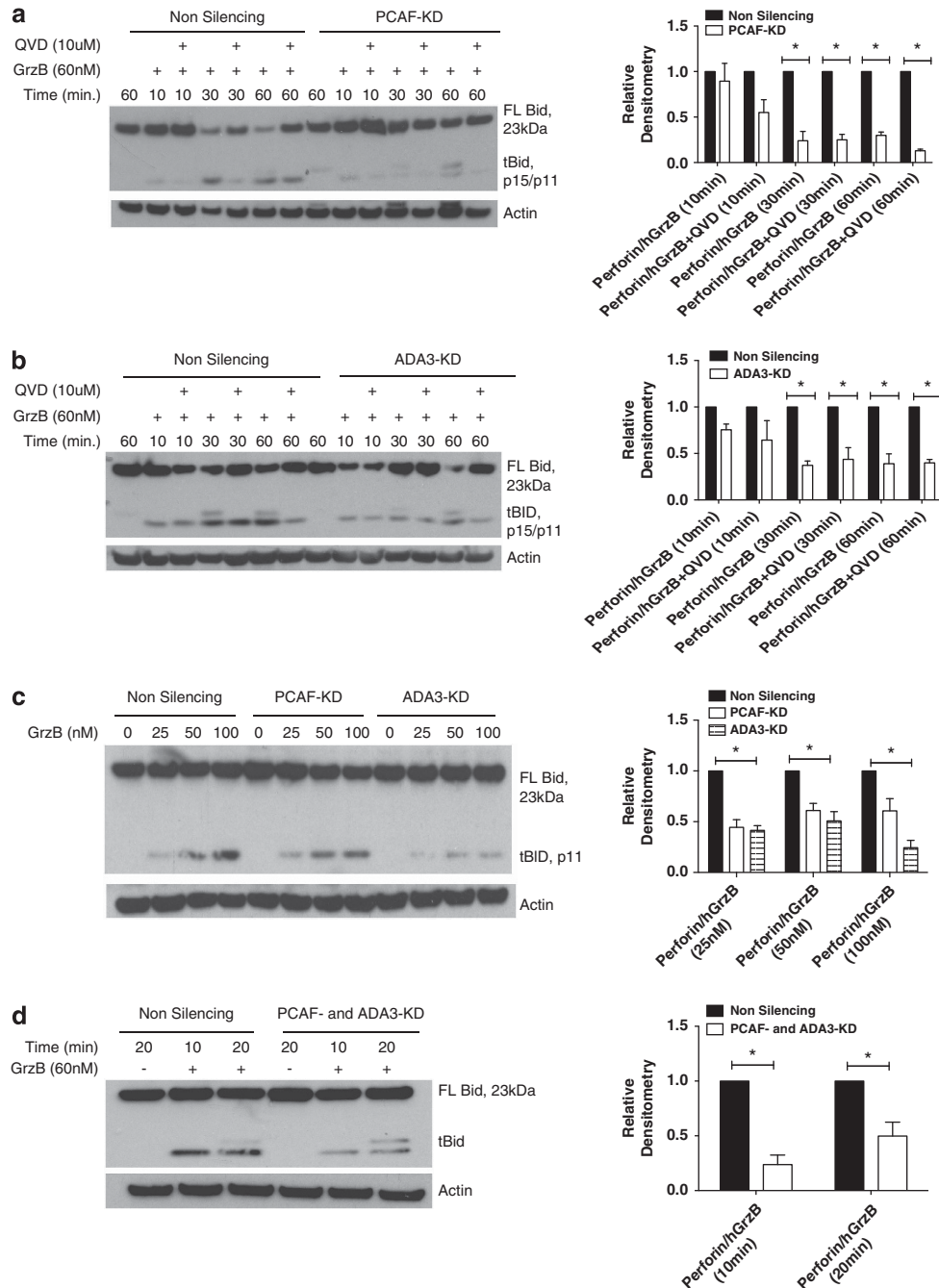


Figure 5 PCAF-KD or ADA3-KD cells have reduced perforin/hGrz-mediated Bid processing. **(a)** PCAF-KD suppresses perforin/hGrzB-mediated Bid processing. Non-silencing or PCAF-KD HeLa were treated for 10, 30 or 60 min with sublytic perforin in the absence or presence of hGrzB (60 nM) and/or QVD (10 uM) and whole-cell lysates were subjected to immunoblot for Bid detecting full length (FL) and cleaved (tBid, p15/p11) with a representative histogram densitometry analysis. Total protein was evaluated by detecting Actin levels. **(b)** ADA3-KD suppresses perforin/hGrzB-mediated Bid processing. Non-silencing or ADA3-KD HeLa were treated for 10, 30 or 60 min with sublytic perforin in the absence or presence of hGrzB (60 nM) and/or QVD (10 uM) and whole-cell lysates were subjected to immunoblot for Bid detecting full length (FL) and cleaved (tBid, p15/p11) with a representative histogram of densitometry analysis. Total protein was evaluated by detecting Actin levels. **(c)** PCAF-KD or ADA3-KD suppress perforin/hGrzB-mediated Bid processing at high concentrations of hGrzB. Non-Silencing, PCAF-KD or ADA3-KD HeLa were treated for 10 min with sublytic perforin in the absence or presence of hGrzB at the indicated concentrations and whole-cell lysates were subjected to immunoblot for Bid detecting full length (FL) and cleaved (tBid, p11) with a representative histogram of densitometry analysis. Total protein was evaluated by detecting Actin levels. **(d)** PCAF- and ADA3-KD suppress perforin/hGrzB-mediated Bid processing. Non-silencing or PCAF- and ADA3-KD HeLa, were treated with sublytic perforin in the absence or presence of hGrzB (60 nM) at the indicated times and total cell lysates were subjected to immunoblot for Bid detecting full length (FL) and cleaved (tBid, p15/p11) with a representative histogram densitometry analysis. Total protein was evaluated by detecting Actin levels. Immunoblots are a representative of three independent experiments, densitometry analysis: a representative of three immunoblots expressed relative to the non-silencing group for each treatment and normalized to the intensity of actin. Error bars represent S.E.M., $n = 3$. Statistical analysis performed: one-way ANOVA versus non-silencing and a Bonferroni test, $*P < 0.05$

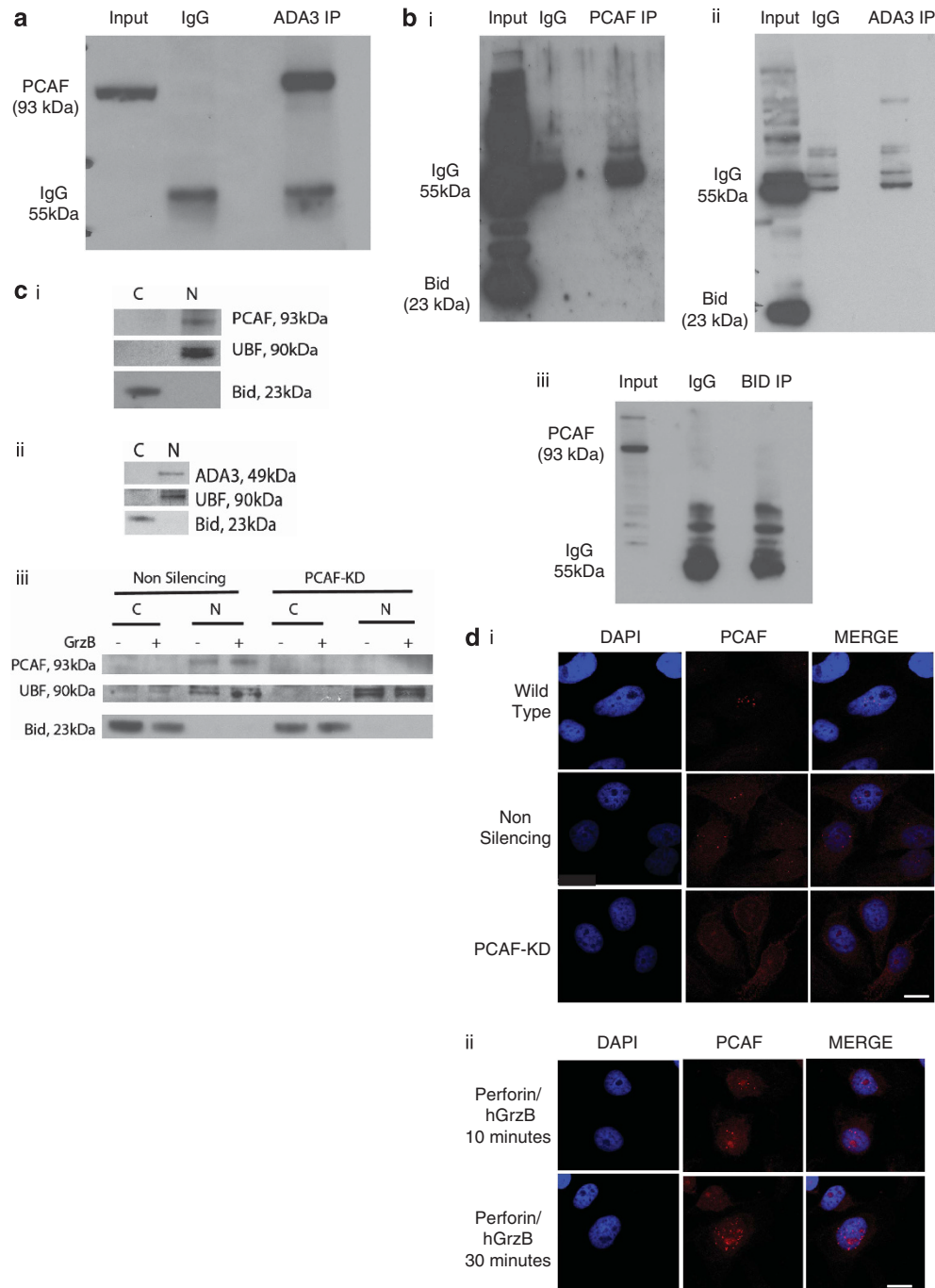


Figure 6 PCAF and ADA3 cooperate directly and are nuclear in localization, but no direct interaction with Bid is observed. HeLa wild-type cell lysates were used for immunoprecipitation (IP) and 10% of the input lysate, total IgG or total IP lysate were subjected to immunoblot and probed for the indicated antibody. The 55 kDa band denotes the IgG heavy weight band. **(a)** PCAF and ADA3 interact directly. Immunoblot for ADA3 IP probed for PCAF. **(b)** Bid does not interact with PCAF or ADA3. **i.** Immunoblot for PCAF IP probed for Bid **ii.** Immunoblot for ADA3 IP probed for Bid and **iii.** Immunoblot for Bid IP probed for PCAF. **(c)** PCAF or ADA3 reside in the nucleus. HeLa WT cells were separated for cytoplasmic (C) and nuclear (N) fractions and lysates were subjected to immunoblot: **i.** Immunoblot probed for PCAF or upstream binding factor (UBF) as a nuclear marker, followed by Bid as a cytosolic marker; **ii.** Immunoblot probed for ADA3, UBF as a nuclear marker and Bid for a cytosolic marker; **iii.** HeLa non-silencing or PCAF-KD cells were treated with sublytic perforin in the absence or presence of hGrzB (60 nM) for 15 min and cytoplasmic (C) and nuclear (N) extracts were isolated and subjected to immunoblot for PCAF, UBF as a nuclear marker and Bid for a cytosolic marker. **(d)** PCAF remains in the nucleus following perforin/hGrzB treatment. **i.** HeLa wild type (WT), non-silencing or PCAF-KD cells were formaldehyde fixed and stained with PCAF followed by DAPI for nuclear staining. Cells were imaged for the localization of PCAF (red) protein and compared with DAPI (blue) nuclear staining by confocal microscopy, scale bars represent 10 μ m. **ii.** HeLa WT cells treated with sublytic perforin/hGrzB (60 nM) for the indicated times were formaldehyde fixed and stained with PCAF followed by DAPI for nuclear staining. Cells were imaged for PCAF (red) protein localization and compared with DAPI (blue) nuclear staining, by confocal microscopy, scale bars represent 10 μ m. Immunoblots and immunofluorescence images are a representative of three independent experiments

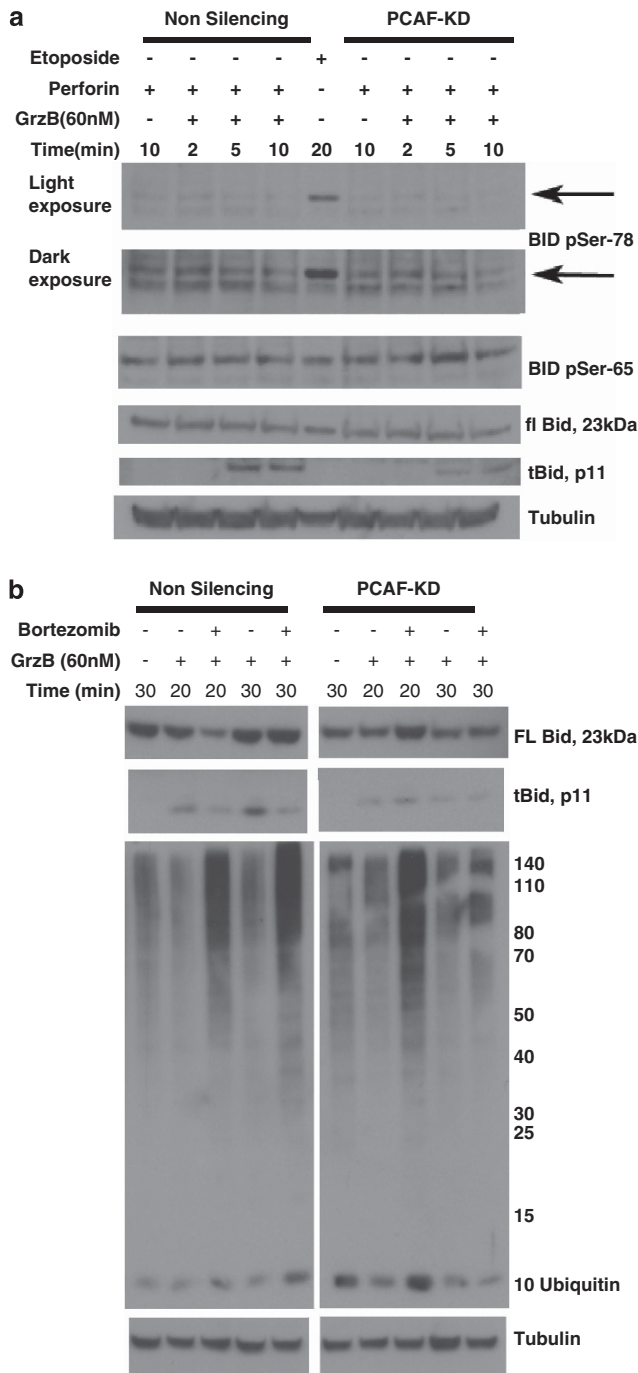


Figure 7 Analysis of Bid modifications in PCAF-depleted cells. (a) The phosphorylation of Bid does not change in PCAF-depleted HeLa. Non-silencing or PCAF-KD cells were treated with sublytic perforin in the absence or presence of hGrzB (60 nM) at the indicated times in minutes ($_{min}$) or etoposide (100 μ M) for 20 min and whole-cell lysates were subjected to immunoblot detecting Bid: phospho-S78 (pSer78); phospho-S65 (pSer65); Bid full length (FL) or cleaved (tBid, p11). Tubulin immunoblot served as loading control. (b) Inhibition of the proteasome, does not alter Bid processing in PCAF-KD HeLa. Non-silencing or PCAF-KD were pre-treated with Bortezomib (1 h, 100 μ M) as indicated, then with sublytic perforin in the absence or presence of hGrzB (60 nM) at the indicated times in minutes ($_{min}$) and whole-cell lysates were subjected to immunoblot for Bid detecting full length (FL) and cleaved Bid (tBid, p11) or Ubiquitin (middle panel). Tubulin immunoblot served as loading control. Immunoblots are a representation of three independent experiments

can be reset to render a target cell more or less sensitive to Bid-mediated MOMP has potential therapeutic implications in cancer. We recently showed that overexpression of Bcl-2 and like inhibitors in tumor cells can potentially be overcome by combining hGrzB and a BH3-mimetic agent such as ABT-737 and that the hGrzB death signal is remarkably long lived.³⁹ The well-described capacity of various human cancers to downregulate PCAF or ADA3 levels^{40–43} would be expected to blunt combination therapies such as this, by repressing the latent pro-apoptotic signal provided by tBid.

The involvement of PCAF and/or ADA3 in disease in normal development and a number of pathologies is well described. ADA3-null mice die *in utero*,⁴⁴ probably due to a defect in cell cycle progression. ADA3 can upregulate the p53 tumor suppressor, while both ADA3 and p53 can be deregulated via the human papillomavirus oncoprotein E6, with implications in many cancers particularly cervical.⁴³ ADA3 can bind to estrogen promoters to recruit histone acetyl transferases including PCAF to enhance receptor expression, consequential in estrogen-dependent tumor cell growth.⁴⁵ Finally, ADA3 can regulate beta-catenin, a transcriptional activator of the Wntless-Int signaling pathway,⁴⁶ de-regulation of which is implicated in various malignancies including acute myeloid leukemia.⁴⁷ In contrast to ADA3, PCAF-null mice develop normally,⁴⁸ but PCAF is implicated in a number of disease states including arteriosclerosis (including aneurysm formation) and Alzheimer's disease.^{49–51} A specific PCAF gene polymorphism has also been linked to hepatocellular carcinoma.⁵² Malignancies associated with BRCA2 gene mutation may be linked to deregulated PCAF recruitment to target genes, leading to disordered cell division and aneuploidy.⁵³ Finally, downregulation of PCAF has been observed in esophageal squamous cell carcinoma, ovarian and colorectal cancer.^{40–42} Exactly how reduced expression and/or function of PCAF and ADA3 might lead to human diseases including cancer remains unclear. Small molecule inhibitors of PCAF have been reported; however, further studies on their specificity and role in disease are warranted^{52,54} as is a further exploration of the potential impact of PCAF/ADA3 on immune-based cancer therapies.

Materials and Methods

Cell culture and reagents. HeLa cells were maintained as previously described.⁵⁵ HCT116 cells were maintained in RPMI (Gibco Life Technologies, Carlsbad, CA, USA) supplemented with 10% fetal bovine serum. For Bcl-2-overexpression, cells were transfected and selected as previously described.¹⁸ For Bid-KD cells, the p-Retro-Super vector containing shRNA for Bid was a gift from Professor J Borst, Netherlands Cancer Institute.⁵⁶ For non-silencing (NS), ADA3-KD and PCAF-KD cells, the pGIPZ vector containing the shRNA targeting NS, ADA3 or PCAF were obtained from Thermo-Fisher Scientific (Franklin, MA, USA). Cells expressing shRNA were selected with puromycin (2 μ g/ml, Sigma-Aldrich, St. Louis, MO, USA) for 48 h and maintained in culture with 1 μ g/ml puromycin for stable cell line continuity. For the shRNA screen a library of ~4000 shRNAs directed against 1213 genes associated with cell death was obtained from Thermo-Fisher Scientific. Embedded shRNAs in an endogenous miR30 microRNA backbone was a major advance over previous shRNA screening vectors as the miR30 structure significantly enhances the shRNA efficiency through increased Drosha and Dicer processing of the expressed hairpins.⁵⁷ The library used in this screen was at the time the most sophisticated resource available for high throughput shRNA screening. Recombinant hGrzB was produced in *Pichia pastoris*⁵⁸

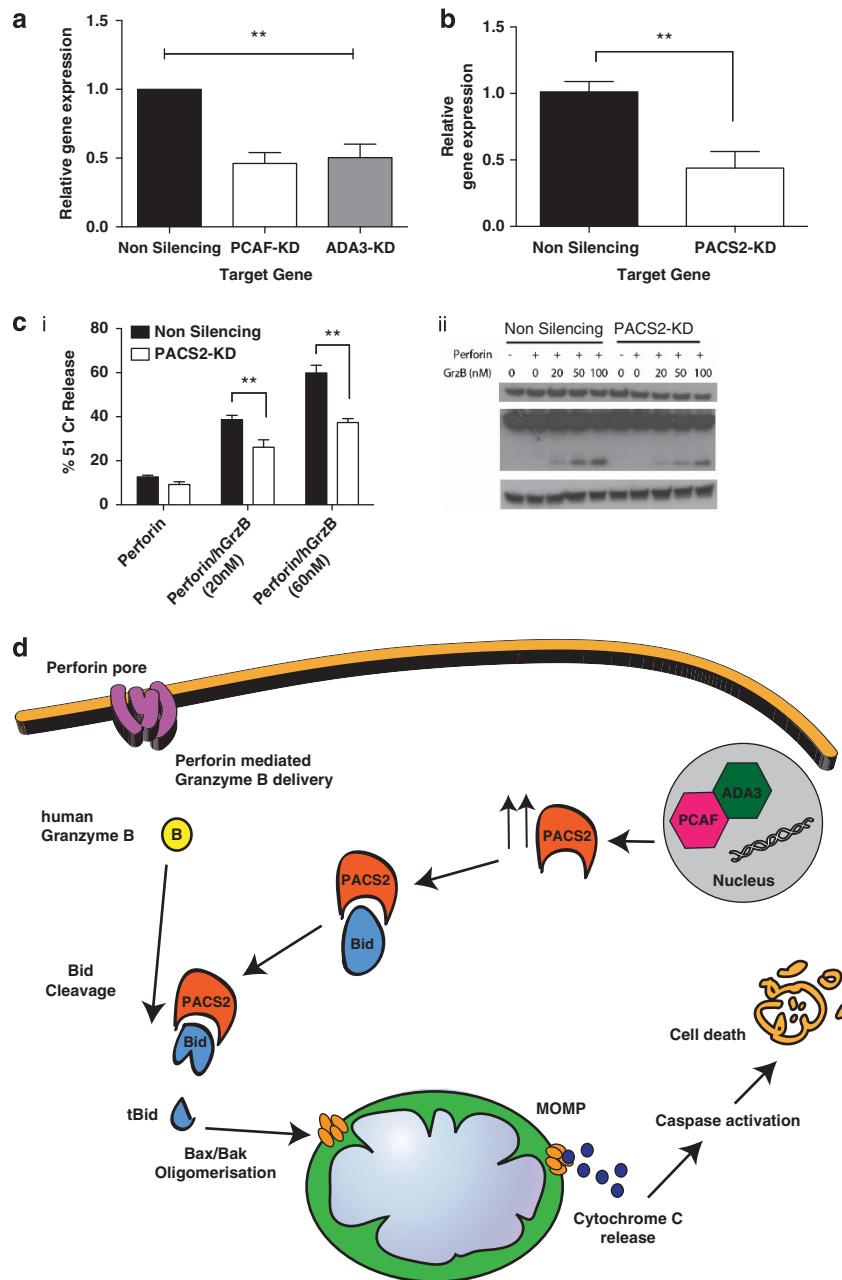


Figure 8 PACS2 depletion in HeLa confers resistance to perforin/hGrzB-mediated cell death and reduced Bid processing. (a) PCAF-KD or ADA3-KD HeLa have reduced PACS2 expression. PCAF-KD, ADA3-KD or non-silencing cells were examined for PACS2 expression by RNA extraction and relative mRNA expression of PACS2 was measured by qRT-PCR. (b) HeLa transfected with PACS2 shRNA have reduced PACS2 expression. RNA was extracted from non-silencing, or PACS2-KD HeLa and relative mRNA expression for PACS2 was detected by qRT-PCR. (c) PACS2-depleted HeLa are resistant to perforin/hGrzB-mediated cell death and have reduced Bid processing. i. PACS2-KD or non-silencing HeLa were treated with sublytic perforin in the absence or presence of hGrzB at 30 nM and 60 nM and a 4 h ^{51}Cr release assay was completed. ii. Non-silencing, or PACS2-KD HeLa were treated for 20 min with sublytic perforin in the absence or presence of hGrzB at the indicated concentrations and whole-cell lysates were subjected to immunoblot for Bid detecting full length (FL) and cleaved (tBid, p11). Total protein was evaluated by detecting Actin levels. (d) A simplified schematic depicting the role that PCAF and ADA3 have in perforin-mediated human perforin/hGrzB-induced cell death and their effect on Bid processing via the transport protein PACS2. The suggested mechanism shows the following: PCAF and ADA3 influence the expression of PACS2; PACS2 binds to full-length Bid and assists in its trafficking and cleavage (tBid) by human GrzB; tBid instigates Bax/Bak oligomerisation which induces mitochondrial outer membrane permeabilisation (MOMP); inducing cytochrome-c release (as well as Smac/Diablo) which activates caspases and leads to cell death. Error bars represent S.E.M., $n = 3$. Statistical analysis performed: one way ANOVA versus non-silencing and a Bonferroni test, $**P < 0.01$

and recombinant mouse perforin was produced in a baculovirus expression system.⁵⁵ For recombinant hGrzB, 20–60 nM was considered low–middle potency. Caspases were blocked with Q-VD-OPh (10 μM , Calbiochem, La Jolla, CA, USA). Human-TRAIL ligand was from Peprotech (Rocky Hill, NJ, USA).

Cells were exposed to UV-light Joules/centimeter² (J/cm^2) using an Ultraviolet Crosslinker (CL1000, UVP, Upland, CA, USA). Cells were treated with 100 μM Bortezomib (Millennium Pharmaceuticals, Cambridge, MA, USA) for 1 h or with 100 μM Etoposide (Pfizer, New York, NY, USA), for 20 min.

Transfections and transductions. For retrovirus production, HEK293T cells were transfected with p-Retro-Super shRNA and pLMP using Fugene-6 according to the manufacturer's instructions (Promega, Madison, WI, USA). For lentivirus production the HEK293T cells were transfected with pGIPZ plasmids (Sequence and Catalog Reference: non-silencing, VGH5518; ADA3, 5'-CCAA GATCCAGGAATATGA-3', V2LHS_253631; PCAF, 5'-CAACTAATATACAAC CATA-3', V2LMM_189282; PCAF-88, 5'-GTACTACGTGCTAAGAAA-3', V2LHS_53088; PCAF-89, 5'-CAAACAAGTTTATTCTAT-3', V2LHS_53089; PCAF-90, 5'-GCCCGAATCGCCGTGAAGA-3', V2LHS_53090; PCAF-91, 5'-CAAGTTTATTCTATCTAT-3' V2LHS_53091; PACS2, 5'-CAGAGATACTG CAACTGCA-3', V2LHS_91559) and LentiX-HT packaging mix (Clontech, Mountain View, CA, USA) using the polyethylenimine (PEI) transfection method, PEI was purchased from PolySciences (Warrington, PA, USA). Forty-eight hours after the transfection, media containing virus was collected and cells were transduced, cultured for 16 h and media was refreshed. Successfully transduced cells were selected with puromycin (2 μ g/ml) for 48 h. For siRNA transfection of cells, the Thermo-Fisher Scientific reverse transfection method was used to transiently transfect cells with siRNA-SMARTPOOL (Thermo-Fisher Scientific) (catalog reference: non-targeting (NT), D-001810; PCAF, L-005055; ADA3, L-017508; GAPDH, D-001830). Briefly, DharmafECT lipid (Thermo-Fisher Scientific) and siRNA were complexed with siRNAs in Opti-MEM (Gibco Life Technologies) for 20 min then mixed with cells in maintenance media. Sixteen hours following transfection, media was refreshed and 24 h following, cells were processed.

Immunoblot analysis. Whole-cell lysates were prepared in NP40 lysis buffer and protein quantification was determined by Coomassie-Bradford (Thermo-Fisher Scientific). Lysates were separated on 4–12% Nu-Page Bis-Tris gradient gels (Invitrogen, Carlsbad, CA, USA) and probed using antibodies to: Bcl-2 (Pharmingen, San Diego, CA, USA); Bid (clone no. 2D1),⁵⁹ Caspase-8 (Pharmingen); Caspase-3 (Pharmingen); PCAF (SantaCruz, Dallas, TX, USA); ADA3 (SantaCruz); Phospho-Bid (S78) (Bethyl Laboratories, Montgomery, TX, USA); Phospho-Bid (S65) (Abcam, Cambridge, MA, USA); Ubiquitin P4D1 (Cell Signaling, San Diego, CA, USA); or SERPIN-B9,²⁶ as previously described.⁶ Identifying and quantifying immunoblots, ImageJ software (ImageJ 1.475v, NIH, USA) was used to measure densitometry.

Immunoprecipitation. Typically 5×10^6 cells were lysed in 1% Triton X-100, 50 mM Tris-HCl pH 8, 300 mM NaCl, 0.02% NaAz containing protease inhibitors (Roche, Basel, Switzerland) for 30 min on ice. Insoluble debris was pelleted and lysates were pre-cleared with 1:1% slurry of sepharose beads in lysis buffer for 1 h at 4 °C. Ten micrograms of antibody for: PCAF (Bethyl Laboratories); Bid (Cell Signaling); ADA3 (SantaCruz); or IgG control, was pre-conjugated to 1:1% slurry of sepharose beads in PBS for 2 h at 4 °C. Lysate was pelleted to remove beads and 10 μ l was stored as input control, and the remaining lysate was subdivided for immunoprecipitation (IP) with IgG control or specific antibody:bead conjugates. IP were performed for 16 h at 4 °C with gentle agitation. Immune complexes were washed four times with wash buffer (0.1% Triton X-100, 50 mM Tris, 300 mM NaCl, 5 mM EDTA, 0.02% NaAz), once with PBS and eluted by boiling in sample buffer and separated on Nu-Page gels as described above.

Cytotoxicity assays. Generally 0.5×10^6 cells were treated at 37 °C with hGrzB at the specified concentration and a concentration of perforin known to induce 10% background lysis. Chromium (⁵¹Cr) and cytochrome c release assays were performed as previously described.^{19,25} For flow cytometry (FACS), cells were washed with PBS containing 0.5% FCS then resuspended in the same solution with 7-AAD-FITC (Beckman Coulter, Brea, CA, USA) and 7-AAD-FITC fluorescence was detected on a cytofluorograph. Alamar blue (AB) exclusion was used according to the manufacturer's instructions (Life Technologies, Grand Island, NY, USA).

RNA isolation and first-strand cDNA synthesis. Total RNA was isolated using the RNeasy mini kit (Qiagen, Germantown, MD, USA) according to the manufacturer's instructions. First-strand cDNA synthesis was performed using M-MLV Reverse Transcriptase (Promega) according to the manufacturer's instructions. HPRT, GAPDH, PCAF, ADA3, Bid, Bcl-2, Bcl-w, Mcl-1, Bcl-xl, PACS2 and SERPIN-B9 genes (primers available on request) were quantified using qPCR. PCR amplification was performed using an ABI Prism-7500

(Life Technologies) with 2 pmol of each primer to 20 μ l of $1 \times$ POWER Sybergreen PCR Mastermix (Life Technologies). Annealing was at 50 °C for 2 min, denaturing at 95 °C for 10 min followed by 40 synthesis cycles at 60 °C for 1 minute.

Cell fractionation. Nuclear extracts from 2×10^6 cells were prepared as follows: cells were washed in ice-cold PBS, resuspended in 400 μ l low salt buffer (10 mM Hepes pH 8, 1.5 mM MgCl₂, 10 mM KCl, 0.5 mM DTT and 0.2 mM PMSF) on ice for 10 min, pelleted and the supernatant put aside (cytosolic extract). The nuclei were gently resuspended in 200 μ l high salt buffer (20 mM Hepes pH 8, 25% glycerol, 420 mM KCl, 1.5 mM MgCl₂, 0.2 mM EDTA, 0.5 mM DTT and 0.2 mM PMSF) and incubated on ice for 30 min. Debris from the nuclear extracts was removed by centrifugation. Lysate concentration was measured by Bradford assay (ThermoFisher Scientific, Rockford, IL, USA) and equal amounts of nuclear and cytoplasmic protein was loaded for immunoblot analysis.

Immunofluorescence microscopy. HeLa cells were plated in eight well chamber slides, rinsed in PBS, fixed with 4% paraformaldehyde and stained as previously described.⁶⁰ Cells were stained with PCAF (Millipore, Billerica, MA, USA) and imaged as previously described.⁶⁰

hGrzB activity assay. hGrzB activity was determined by the hydrolysis of synthetic peptide thiobenzylester substrate (Asp-ase activity, Boc-Ala-Ala-Asp-S-Bzl; SM Biochemicals), as previously described.¹

Intracellular hGrzB staining. HeLa were treated with hGrzB (60 nM) in the absence or presence of perforin (1 nM) for the indicated times, fixed, permeabilized and stained with a PE-labeled hGrzB antibody (Clone GB11, Sanquin, Amsterdam, The Netherlands). GrzB-PE was detected on a cytofluorograph.

Statistical analysis. Results are presented as mean \pm S.E.M. Statistical differences for different treatments were evaluated by using t-test or one-way ANOVA with Bonferroni adjustment by Prism software (GraphPad, La Jolla, CA, USA). A P-value of < 0.05 was considered significant.

Conflict of Interest

The authors declare no conflict of interest.

Acknowledgements. This study was supported by Program, Fellowship and Project grant support from the National Health and Medical Research Council (NHMRC) of Australia and the Cancer Council Victoria.

1. Kaiserman D, Bird CH, Sun J, Matthews A, Ung K, Whisstock JC *et al*. The major human and mouse granzymes are structurally and functionally divergent. *J Cell Biol* 2006; **175**: 619–630.
2. Kagi D, Ledermann B, Burki K, Seiler P, Odermatt B, Olsen KJ *et al*. Cytotoxicity mediated by T cells and natural killer cells is greatly impaired in perforin-deficient mice. *Nature* 1994; **369**: 31–37.
3. Heibein JA, Goping IS, Barry M, Pinkoski MJ, Shore GC, Green DR *et al*. Granzyme B-mediated cytochrome c release is regulated by the Bcl-2 family members bid and Bax. *J Exp Med* 2000; **192**: 1391–1402.
4. Barry M, Heibein JA, Pinkoski MJ, Lee SF, Moyer RW, Green DR *et al*. Granzyme B short-circuits the need for caspase 8 activity during granule-mediated cytotoxic T-lymphocyte killing by directly cleaving Bid. *Mol Cell Biol* 2000; **20**: 3781–3794.
5. Alimonti JB, Shi L, Baijal PK, Greenberg AH. Granzyme B induces BID-mediated cytochrome c release and mitochondrial permeability transition. *J Biol Chem* 2001; **276**: 6974–6982.
6. Sutton VR, Davis JE, Cancilla M, Johnstone RW, Ruefli AA, Sedelies K *et al*. Initiation of apoptosis by granzyme B requires direct cleavage of bid, but not direct granzyme B-mediated caspase activation. *J Exp Med* 2000; **192**: 1403–1414.
7. Degli Esposti M, Ferry G, Masdehors P, Boutin JA, Hickman JA, Dive C. Post-translational modification of Bid has differential effects on its susceptibility to cleavage by caspase 8 or caspase 3. *J Biol Chem* 2003; **278**: 15749–15757.
8. Sutton VR, Vaux DL, Trapani JA. Bcl-2 prevents apoptosis induced by perforin and granzyme B, but not that mediated by whole cytotoxic lymphocytes. *J Immunol* 1997; **158**: 5783–5790.
9. Davis JE, Sutton VR, Smyth MJ, Trapani JA. Dependence of granzyme B-mediated cell death on a pathway regulated by Bcl-2 or its viral homolog, BHRF1. *Cell Death Differ* 2000; **7**: 973–983.

10. Cullen SP, Adrain C, Luthi AU, Duriez PJ, Martin SJ. Human and murine granzyme B exhibit divergent substrate preferences. *J Cell Biol* 2007; **176**: 435–444.
11. Lopez JA, Jenkins MR, Rudd-Schmidt JA, Brennan AJ, Danne JC, Mannering SI *et al*. Rapid and unidirectional perforin pore delivery at the cytotoxic immune synapse. *J Immunol* 2013; **191**: 2328–2334.
12. Browne KA, Johnstone RW, Jans DA, Trapani JA. Filamin (280-kDa actin-binding protein) is a caspase substrate and is also cleaved directly by the cytotoxic T lymphocyte protease granzyme B during apoptosis. *J Biol Chem* 2000; **275**: 39262–39266.
13. Martin P, Pardo J, Schill N, Jockel L, Berg M, Froelich CJ *et al*. Granzyme B-induced and caspase 3-dependent cleavage of gelsolin by mouse cytotoxic T cells modifies cytoskeleton dynamics. *J Biol Chem* 2010; **285**: 18918–18927.
14. Sebbagh M, Hamelin J, Bertoglio J, Solary E, Breard J. Direct cleavage of ROCK II by granzyme B induces target cell membrane blebbing in a caspase-independent manner. *J Exp Med* 2005; **201**: 465–471.
15. Schiltz RL, Nakatani Y. The PCAF acetylase complex as a potential tumor suppressor. *Biochim Biophys Acta* 2000; **1470**: M37–M53.
16. Yang XJ, Ogrzyko VV, Nishikawa J, Howard BH, Nakatani Y. A p300/CBP-associated factor that competes with the adenoviral oncoprotein E1A. *Nature* 1996; **382**: 319–324.
17. Spedale G, Timmers HT, Pijnappel WW. ATAC-king the complexity of SAGA during evolution. *Genes Dev* 2012; **26**: 527–541.
18. Pinkoski MJ, Waterhouse NJ, Heibin JA, Wolf BB, Kuwana T, Goldstein JC *et al*. Granzyme B-mediated apoptosis proceeds predominantly through a Bcl-2-inhibitable mitochondrial pathway. *J Biol Chem* 2001; **276**: 12060–12067.
19. Waterhouse NJ, Trapani JA. A new quantitative assay for cytochrome c release in apoptotic cells. *Cell Death Differ* 2003; **10**: 853–855.
20. Yan W, Huang JX, Lax AS, Pelliniemi L, Salminen E, Poutanen M *et al*. Overexpression of Bcl-W in the testis disrupts spermatogenesis: revelation of a role of BCL-W in male germ cell cycle control. *Mol Endocrinol* 2003; **17**: 1868–1879.
21. Pritchard DM, Print C, O'Reilly L, Adams JM, Potten CS, Hickman JA. Bcl-w is an important determinant of damage-induced apoptosis in epithelia of small and large intestine. *Oncogene* 2000; **19**: 3955–3959.
22. Fulda S, Meyer E, Debatin KM. Inhibition of TRAIL-induced apoptosis by Bcl-2 overexpression. *Oncogene* 2002; **21**: 2283–2294.
23. MacFarlane M, Morrison W, Dinsdale D, Cohen GM. Active caspases and cleaved cytokeratins are sequestered into cytoplasmic inclusions in TRAIL-induced apoptosis. *J Cell Biol* 2000; **148**: 1239–1254.
24. Slee EA, Keogh SA, Martin SJ. Cleavage of BID during cytotoxic drug and UV radiation-induced apoptosis occurs downstream of the point of Bcl-2 action and is catalysed by caspase-3: a potential feedback loop for amplification of apoptosis-associated mitochondrial cytochrome c release. *Cell Death Differ* 2000; **7**: 556–565.
25. Waterhouse NJ, Sedelies KA, Browne KA, Wowk ME, Newbold A, Sutton VR *et al*. A central role for Bid in granzyme B-induced apoptosis. *J Biol Chem* 2005; **280**: 4476–4482.
26. Bird CH, Sutton VR, Sun J, Hirst CE, Novak A, Kumar S *et al*. Selective regulation of apoptosis: the cytotoxic lymphocyte serpin proteinase inhibitor 9 protects against granzyme B-mediated apoptosis without perturbing the Fas cell death pathway. *Mol Cell Biol* 1998; **18**: 6387–6398.
27. Blanco-Garcia N, Asensio-Juan E, de la Cruz X, Martinez-Balbas MA. Autoacetylation regulates P/CAF nuclear localization. *J Biol Chem* 2009; **284**: 1343–1352.
28. Desagher S, Osen-Sand A, Montessuit S, Magnenat E, Vilbois F, Hochmann A *et al*. Phosphorylation of bid by casein kinases I and II regulates its cleavage by caspase 8. *Mol Cell* 2001; **8**: 601–611.
29. Kamer I, Sarig R, Zaltsman Y, Niv H, Oberkovitz G, Regev L *et al*. Proapoptotic BID is an ATM effector in the DNA-damage response. *Cell* 2005; **122**: 593–603.
30. Korsmeyer SJ, Wei MC, Saito M, Weiler S, Oh KJ, Schlesinger PH. Pro-apoptotic cascade activates BID, which oligomerizes BAK or BAX into pores that result in the release of cytochrome c. *Cell Death Differ* 2000; **7**: 1166–1173.
31. Simmen T, Aslan JE, Blagoveshchenskaya AD, Thomas L, Wan L, Xiang Y *et al*. PACS-2 controls endoplasmic reticulum–mitochondria communication and Bid-mediated apoptosis. *EMBO J* 2005; **24**: 717–729.
32. Sheridan JP, Marsters SA, Pitti RM, Gurney A, Skubatch M, Baldwin D *et al*. Control of TRAIL-induced apoptosis by a family of signaling and decoy receptors. *Science* 1997; **277**: 818–821.
33. Scaffidi C, Fulda S, Srinivasan A, Friesen C, Li F, Tomaselli KJ *et al*. Two CD95 (APO-1/Fas) signaling pathways. *EMBO J* 1998; **17**: 1675–1687.
34. Linares LK, Kiernan R, Triboulet R, Chable-Bessia C, Latreille D, Cuvier O *et al*. Intrinsic ubiquitination activity of PCAF controls the stability of the oncoprotein Hdm2. *Nat Cell Biol* 2007; **9**: 331–338.
35. Susanto O, Stewart SE, Voskoboinik I, Brasacchio D, Hagn M, Ellis S *et al*. Mouse granzyme A induces a novel death with writhing morphology that is mechanistically distinct from granzyme B-induced apoptosis. *Cell Death Differ* 2013; **20**: 1183–1193.
36. Quan LT, Caputo A, Bleackley RC, Pickup DJ, Salvesen GS. Granzyme B is inhibited by the cowpox virus serpin cytokine response modifier A. *J Biol Chem* 1995; **270**: 10377–10379.
37. Andrade F, Casciola-Rosen LA, Rosen A. A novel domain in adenovirus L4-100K is required for stable binding and efficient inhibition of human granzyme B: possible interaction with a species-specific exosite. *Mol Cell Biol* 2003; **23**: 6315–6326.
38. Medema JP, de Jong J, Peltenburg LT, Verdegaaal EM, Gorter A, Bres SA *et al*. Blockade of the granzyme B/perforin pathway through overexpression of the serine protease inhibitor PI-9/SPI-6 constitutes a mechanism for immune escape by tumors. *Proc Natl Acad Sci USA* 2001; **98**: 11515–11520.
39. Sutton VR, Sedelies K, Dewson G, Christensen ME, Bird PI, Johnstone RW *et al*. Granzyme B triggers a prolonged pressure to die in Bcl-2 overexpressing cells, defining a window of opportunity for effective treatment with ABT-737. *Cell Death Dis* 2012; **3**: e344.
40. Zhu C, Qin YR, Xie D, Chua DT, Fung JM, Chen L *et al*. Characterization of tumor suppressive function of P300/CBP-associated factor at frequently deleted region 3p24 in esophageal squamous cell carcinoma. *Oncogene* 2009; **28**: 2821–2828.
41. Sunde JS, Donniger H, Wu K, Johnson ME, Pestell RG, Rose GS *et al*. Expression profiling identifies altered expression of genes that contribute to the inhibition of transforming growth factor-beta signaling in ovarian cancer. *Cancer Res* 2006; **66**: 8404–8412.
42. Giannini R, Cavallini A. Expression analysis of a subset of co-regulators and three nuclear receptors in human colorectal carcinoma. *Anticancer Res* 2005; **25**: 4287–4292.
43. Kumar A, Zhao Y, Meng G, Zeng M, Srinivasan S, Delmolino LM *et al*. Human papillomavirus oncoprotein E6 inactivates the transcriptional coactivator human ADA3. *Mol Cell Biol* 2002; **22**: 5801–5812.
44. Mohibi S, Gurumurthy CB, Nag A, Wang J, Mirza S, Mian Y *et al*. Mammalian alteration/deficiency in activation 3 (Ada3) is essential for embryonic development and cell cycle progression. *J Biol Chem* 2012; **287**: 29442–29456.
45. Germaniuk-Kurowska A, Nag A, Zhao X, Dimri M, Band H, Band V. Ada3 requirement for HAT recruitment to estrogen receptors and estrogen-dependent breast cancer cell proliferation. *Cancer Res* 2007; **67**: 11789–11797.
46. Yang M, Waterman ML, Brachmann RK. hADA2a and hADA3 are required for acetylation, transcriptional activity and proliferative effects of beta-catenin. *Cancer Biol Ther* 2008; **7**: 120–128.
47. Clevers H, Nusse R. Wnt/beta-catenin signaling and disease. *Cell* 2012; **149**: 1192–1205.
48. Yamauchi T, Yamauchi J, Kuwata T, Tamura T, Yamashita T, Bae N *et al*. Distinct but overlapping roles of histone acetylase PCAF and of the closely related PCAF-B/GCN5 in mouse embryogenesis. *Proc Natl Acad Sci USA* 2000; **97**: 11303–11306.
49. Park SY, Lee YH, Seong AR, Lee J, Jun W, Yoon HG. Selective inhibition of PCAF suppresses microglial-mediated beta-amyloid neurotoxicity. *Int J Mol Med* 2013; **32**: 469–475.
50. Gomez D, Kessler K, Michel JB, Vranckx R. Modifications of chromatin dynamics control the Smad2 pathway activation in aneurysmal smooth muscle cells. *Circ Res* 2013; **113**: 881–890.
51. Bastiaansen AJ, Ewing MM, de Boer HC, van der Pouw Kraan TC, de Vries MR, Peters EA *et al*. Lysine acetyltransferase PCAF is a key regulator of arteriogenesis. *Arterioscler, Thromb Vasc Biol* 2013; **33**: 1902–1910.
52. Akil A, Ezzikouri S, El Feydi AE, Benazzoum M, Affif R, Diagne AG *et al*. Associations of genetic variants in the transcriptional coactivators EP300 and PCAF with hepatocellular carcinoma. *Cancer Epidemiol* 2012; **36**: e300–e305.
53. Choi E, Park PG, Lee HO, Lee YK, Kang GH, Lee JW *et al*. BRCA2 fine-tunes the spindle assembly checkpoint through reinforcement of BubR1 acetylation. *Dev Cell* 2012; **22**: 295–308.
54. Ghizzoni M, Boltjes A, Graaf C, Haisma HJ, Dekker FJ. Improved inhibition of the histone acetyltransferase PCAF by an anacardic acid derivative. *Bioorg Med Chem* 2010; **18**: 5826–5834.
55. Sedelies KA, Ciccone A, Clarke CJ, Oliaro J, Sutton VR, Scott FL *et al*. Blocking granule-mediated death by primary human NK cells requires both protection of mitochondria and inhibition of caspase activity. *Cell Death Differ* 2008; **15**: 708–717.
56. Maas C, Verbrugge I, de Vries E, Savich G, van de Kooij LW, Tait SW *et al*. Smac/DIABLO release from mitochondria and XIAP inhibition are essential to limit clonogenicity of Type I tumor cells after TRAIL receptor stimulation. *Cell Death Differ* 2010; **17**: 1613–1623.
57. Silva JM, Li MZ, Chang K, Ge W, Golding MC, Rickles RJ *et al*. Second-generation shRNA libraries covering the mouse and human genomes. *Nat Genet* 2005; **37**: 1281–1288.
58. Sun J, Bird CH, Buzza MS, McKee KE, Whisstock JC, Bird PI. Expression and purification of recombinant human granzyme B from *Pichia pastoris*. *Biochem Biophys Res Commun* 1999; **261**: 251–255.
59. Kaufmann T, Tai L, Ekert PG, Huang DC, Norris F, Lindemann RK *et al*. The BH3-only protein bid is dispensable for DNA damage- and replicative stress-induced apoptosis or cell-cycle arrest. *Cell* 2007; **129**: 423–433.
60. Brennan AJ, Chia J, Browne KA, Ciccone A, Ellis S, Lopez JA *et al*. Protection from endogenous perforin: glycans and the C terminus regulate exocytic trafficking in cytotoxic lymphocytes. *Immunity* 2011; **34**: 879–892.

Supplementary Information accompanies this paper on Cell Death and Differentiation website (<http://www.nature.com/cdd>)